

Article

Features of Metal Hydrogenation during Electron Irradiation

Vitaliy Larionov ¹, Yuriy Tyurin ¹, Tatyana Murashkina ^{1,*} and Thorsteinn Sigfusson ²

¹ School of Nuclear Science & Engineering, National Research Tomsk Polytechnic University, 30 Lenin Avenue, Tomsk 634050, Russian; lvv@tpu.ru (V.L.); tyurin@tpu.ru (Y.T.)

² Iceland Innovation Center, Árleynir 2-8, 112 Reykjavík, Iceland; this@simnet.is

* Correspondence: tatyanaivolokitina@gmail.com; Tel.: +7-960-976-2835

Received: 29 March 2018; Accepted: 20 May 2018; Published: 22 May 2018



Abstract: This paper considers metal hydrogenation and hydrogen release from metals under electron irradiation. The study shows that there are two processes during irradiation: the increase in the hydrogen yield from metal and the increase in the ability of hydrogenated metal to accumulate the energy of a beam of accelerated electrons. The energy introduced into hydrogenated metal is preserved for a longer period when compared to pure metal in time scales of electronic relaxation. Electron irradiation accelerates the saturation of metals with hydrogen and deuterium. Deuterium and hydrogen participate in the collective excitation of the internal hydrogen atmosphere of metals. This effect is explained by the nonequilibrium migration and release of hydrogen from metals. The migration of hydrogen isotopes during irradiation can be used to enhance the light isotope separation.

Keywords: electron irradiation; electron beam; deuterium; palladium; titanium

1. Introduction

Hydrogenated metals are known to be irradiated with electrons, gamma, and X-ray quanta to obtain a radiation-stimulated yield of hydrogen and to excite a hydrogen subsystem. The irradiation of hydrogenated metals by X-rays and electrons [1–7] leads to the long-time excitation of a hydrogen subsystem on the scale of the lifetime of electronic excitations in a metal. The main characteristics of the hydrogen subsystem are the energy, the special state of electrons found in the study of electronic spectra of metals [1,2], and the rate of hydrogen desorption from metals [5]. Irradiation can be used to control the concentration of hydrogen in the volume of solids and to create nonequilibrium thermodynamic systems, the synthesis of which cannot be conducted using traditional methods [4,5]. The study of deuterium desorption from the combined system Pd/PdO saturated with deuterium to form Pd/PdO:D_x and irradiated by electrons has shown that the energy of deuterons increases in comparison to thermal energy [6–8].

High-energy hydrogen (deuterium) atoms are obtained during the excitation of the hydrogen subsystem by electron irradiation due to the generation of plasma oscillations (plasmons) in a crystal lattice or hydrogen subsystem [9,10]. At the same time, some works are devoted to the theoretical justification of the effects of the excitation of the hydrogen subsystem [11]. The important problem is an increase in the time of the preservation of the supplied energy during electronic relaxation in metals to stimulate the processes of accelerated diffusion and the rearrangement of the entire crystal structure exposed to radiation [11–14]. The analysis of oxide films on the surface of metallic samples occupies a special place in the study of hydrogenation conditions. In some cases; their thickness determines the accumulating role of hydrogen, as it delays its output [10,15,16]. Studies of metal

nonequilibrium saturation with hydrogen isotopes result from the needs of high-technology industries such as hydrogen, nuclear, and thermonuclear power industries [17].

The purpose of this work is to study the specific features of the electrolytic accumulation of hydrogen isotopes by using titanium, palladium, and the absorption of hydrogen isotopes, and to obtain the quantitative characteristics for the sorption and desorption of hydrogen isotopes during irradiation.

2. Results and Discussion

Figure 1 shows the kinetic curves demonstrating the change in the deuterium flow passing through a palladium film with a thickness of 0.1 mm. For all electrolyte currents, the value of the flow becomes constant after 260–320 s. The largest deuterium flow is observed for the electrolysis current density of 1 A/cm².

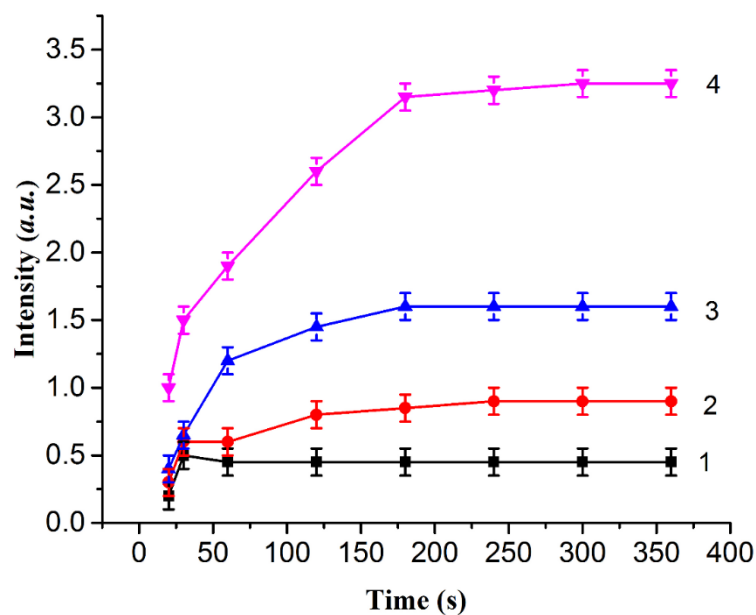


Figure 1. Kinetic curves demonstrating the increase in the density of the deuterium flow passing through palladium (in arbitrary unit) for the different electrolyte current densities: 500 (1), 700 (2), 800 (3), and 1000 mA/cm² (4).

Figure 2 reflects the deuterium flow versus the current density of the electron beam. The relative increment increases superlinearly from the level of excitation by electrons and does not depend on the electrolysis current. The temperature of the electrolyte and Pd of the membrane is kept constant.

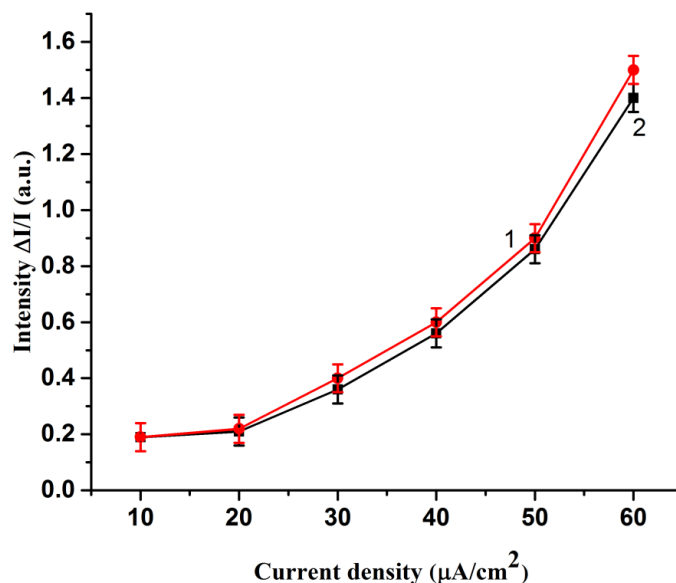


Figure 2. Relative increments of the outgoing deuterium flux density at different current densities of the electron beam ($0 \leq j_e \leq 60 \mu\text{A}$) and two values of the electrolysis current density: 500 (1) and 800 (2) $\mu\text{A}/\text{cm}^2$.

A near-linear dependence was found for the amount of accumulated hydrogen isotopes versus the saturation time (Figure 3). The amount of hydrogen introduced is 2 times greater than the amount of deuterium introduced under similar conditions for the same time. When the electrolysis current is switched on, the instantaneous deuterium yield is not observed in the vacuum cell. The yield of deuterium is observed after 1 h for the Ti samples with a 0.05 mm thickness and after 1 min for the Pd samples with a 0.1 mm thickness, for an electrolysis current density of ca. 200 mA/cm² in D₂O-based alkaline electrolyte (0.1N LiOD) at the electrolyte temperature of 40 °C. This corresponds to the diffusion coefficients of $7 \times 10^{-9} \text{ cm}^2/\text{s}$ (D-Ti) and of $2 \times 10^{-6} \text{ cm}^2/\text{s}$ (D-Pd) at 40 °C.

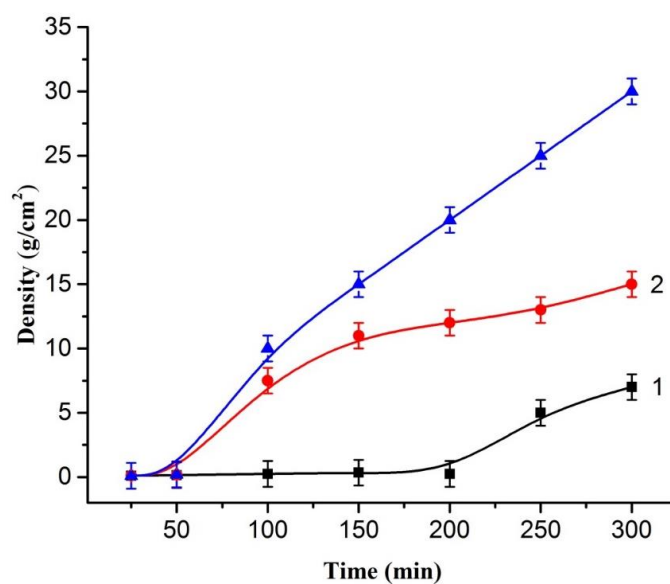


Figure 3. The amount of accumulated deuterium (curves 1 and 2) and hydrogen (3) versus the saturation time ($J = 0.5 \text{ A}/\text{cm}^2$) for palladium (1) and titanium (2 and 3).

Figure 4 shows a decrease in the yield of deuterium for the oxide film 150 nm in thickness and an irradiation time interval of 20 min. Thus, an increase in the thickness of the surface oxide film (Figure 4) leads to a decrease in the rate of the deuterium yield (in a time interval of 15–20 min). In addition, the deuterium yield is increased with an increase in the beam current and a decrease in the temperature. The latter is explained by the fact that there are difficulties connected with the transition of deuterium from the near-surface region to the sample volume. This leads to a higher excitation density of deuterium in the near-surface region and, correspondingly, to an increase in the yield of deuterium.

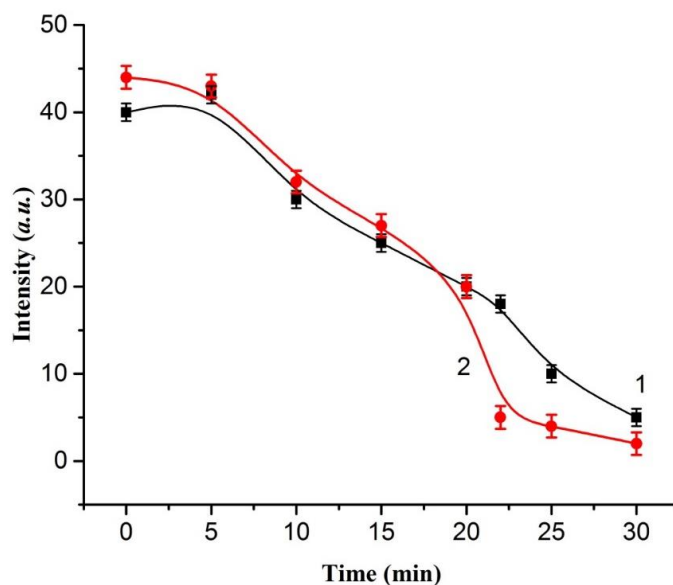


Figure 4. Intensity of the deuterium yield from a palladium sample with an oxide film on the palladium surface (the oxide film thicknesses are 50 nm (1) and 150 nm (2)) versus the irradiation time. The energy of the electron beam is 50 keV, and the beam current is 30–60 μA .

The yield of Li is observed in 1.5–2 h of electrolysis in the alkaline electrolyte (0.1N LiOD) in D_2O on the vacuum side of Pd. Li passes through Pd with a diffusion coefficient of about $D_{\text{Li-Pd}} = 3 \times 10^{-9} \text{ cm}^2/\text{s}$. This diffusion coefficient corresponds to the temperature $T \approx 330 \text{ K}$ and the current of the electron beam $I \approx 60 \mu\text{A}$ (the energy of the electron beam is $E = 50 \text{ keV}$). After the electron irradiation ($J = 30 \mu\text{A}/\text{cm}^2$), up to 90% of hydrogen can be extracted from the palladium samples. Hydrogen is not removed from the samples exposed to X-rays ($E_p = 40$ and 120 keV).

3. Materials and Methods

The palladium (99.9% purity) and α -titanium BT1-0 samples with a composition of Fe 0.18%, Si 0.1%, C 0.07%, O 0.12%, N 0.04%, and H 0.01% were prepared for the study. Palladium 0.1 mm in thickness and titanium 0.05 mm in thickness were used as saturated and simultaneously irradiated samples. After a mechanical polishing, the samples were annealed in a vacuum. The hydrogen concentration was measured using a weight method, a hydrogen analyzer RHEN602 (LECO), and a time-of-flight mass-spectrometer according to the intensity of hydrogen and deuterium lines.

To saturate titanium and palladium with deuterium, electrolysis was used in the 0.3 M solution of LiOD in heavy water with a Pt anode at an electrolysis current density of $j = 10 \text{ mA}/\text{cm}^2$ and a temperature of ca. 279 K. To obtain reproducible experimental gas release results, before electrolysis, the surface of the samples was purified for 20 min from impurities in a UHF discharge plasma at a temperature of 40 °C, a mixture pressure ($\text{H} + \text{H}_2$) of 10 Pa, and for a plasma dissociation degree of ca. 10%. The samples were annealed in a vacuum before electrolysis until the gas release stopped. After electrolytic purifying, the surfaces of the samples were retreated in a low-temperature

hydrogen high-frequency discharge plasma. The electrolytic saturation of titanium was conducted for one hour at an electrolysis current density of $j = 1 \text{ A/cm}^2$; the electrolytic saturation of palladium was conducted for 30 min at an electrolysis current density of $j = 10\text{--}100 \text{ mA/cm}^2$. The content of hydrogen and deuterium in the metals after hydrogenation was determined by both the weight method and mass spectrometry. The migration and yield of deuterium and hydrogen from titanium and palladium exposed to accelerated electrons were studied using mass spectrometry and a high-vacuum installation ($P_{\text{res}} \leq 10^{-5}\text{--}10^{-6} \text{ Pa}$). The installation includes: a vacuum cell, an electron gun, and a mass spectrometer. An electron beam with an energy of 10–100 keV and a current density from 3–150 $\mu\text{A/cm}^2$ was used to create a nonequilibrium yield of hydrogen isotopes. The test sample was placed in a vacuum chamber.

To study the processes of nonequilibrium migration and the escape of hydrogen and deuterium from metals, a special cell is used. It provides electrolytic saturation of metals with H and D atoms with the output of H, D atoms directly into the measuring vacuum chamber (Figure 5). The yield of H, D atoms was stimulated by accelerated electrons ($E = 1\text{--}100 \text{ keV}$, $j_e = 1\text{--}150 \mu\text{A/cm}^2$) or by X-ray radiation ($E_x = 1.0\text{--}100 \text{ keV}$, $j_x = 10^{13}\text{--}10^{15} \text{ quantum}/(\text{cm}^2\text{s})$).

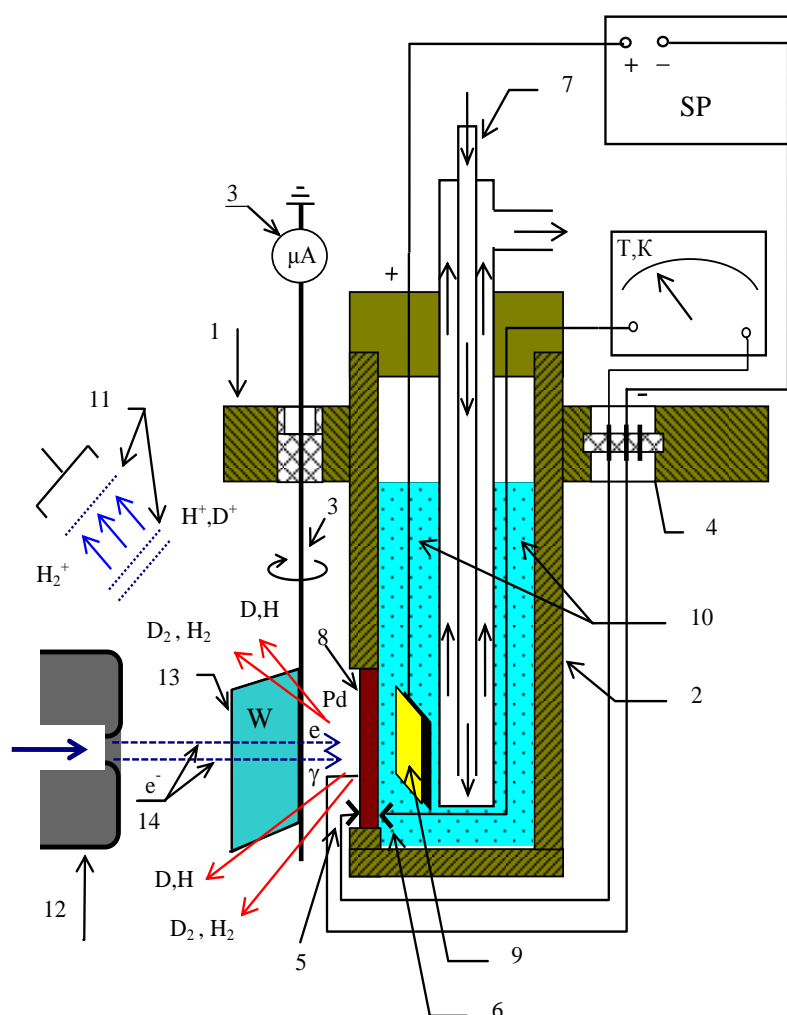


Figure 5. Cell for studying in situ processes of nonequilibrium migration of hydrogen and deuterium in metals: 1—flange; 2—a glass for electrolysis; 3—microammeter for measuring the electron beam current; 4—vacuum current leads; 5, 6—thermocouples; 7—flowing refrigerator; 8—test sample; 9—platinum electrode; 10—electrolyte; 11—mass spectrometer; 12—electron gun; 13—tungsten plate; 14—electron gun; and 15—the cell’s power supply.

The cell allows one to study the electrolytic saturation of metallic samples with hydrogen (deuterium), the passage of hydrogen (deuterium) through the metal and the yield of hydrogen (deuterium) into the vacuum. The passage and exit of hydrogen (deuterium) into the vacuum was stimulated by an electron beam and X-ray radiation. The registration of the H and D atoms was carried out by a time-of-flight mass spectrometer. A beam of accelerated electrons was directed and focused on a saturable sample or transformed into an X-ray beam after passing a tungsten plate.

4. Conclusions

The flows of deuterium and hydrogen were investigated versus the current density of the electron beam, the irradiation time, and the presence of oxide films on the metal surface during electrolysis and the simultaneous irradiation of palladium and titanium. The flow passing through the metal samples and the saturation of the samples was also investigated. A near-linear dependence was found for the amount of accumulated hydrogen isotopes versus the saturation time. The amount of hydrogen introduced is nearly 2 times greater than the amount of deuterium introduced under similar conditions for the same time.

After electron irradiation ($J = 30 \mu\text{A}/\text{cm}^2$), up to 90% of the hydrogen is extracted from the palladium samples, and hydrogen is not removed in significant quantities from the samples exposed to X-rays ($E_p = 40 \text{ keV}$ and 120 keV).

Lithium diffuses through palladium with a diffusion coefficient $D_{\text{Li-Pd}} = 3 \times 10^{-9} \text{ cm}^2/\text{s}$ at a temperature of $T \approx 330 \text{ K}$ and a power density of the electron beam of $\approx 5 \text{ W}/\text{cm}^2$.

The intensity of the hydrogen output from the metal is determined by the linear dependence on the power density of the electron beam.

Author Contributions: V.L. carried out electron irradiation, analyzed the results, and prepared the paper. Y.T. performed the hydrogen removal by an electron beam under different parameters, analyzed the results, and prepared the paper. T.M. performed hydrogenation of the samples and prepared the manuscript. T.S. analyzed the results and prepared the paper. All authors have read and approved the final manuscript.

Acknowledgments: The research was funded by the Tomsk Polytechnic University Competitiveness Enhancement Program.

Conflicts of Interest: The authors declare no conflict of interest.

References

1. Alefeld, G.; Völkl, J. *Hydrogen in Metals I-Basic Properties*; Springer-Verlag: Berlin, Germany, 1978.
2. Elias, R.J.; Corso, H.L.; Gervasoni, J.L. Fundamental aspects of the Ti–H system: Theoretical and experimental behaviour. *Int. J. Hydrog. Energy* **2002**, *27*, 91–97. [[CrossRef](#)]
3. Evard, E.A.; Gabis, I.E.; Voyt, A.P. Study of the kinetics of hydrogen sorption and desorption from titanium. *J. Alloys Compd.* **2005**, *404*, 335–338. [[CrossRef](#)]
4. Scholz, J.; Züchner, H.; Paulus, H.; Müller, K.H. Ion bombardment induced segregation effects in VDX studied by SIMS and SNMS. *J. Alloys Compd.* **1997**, *253*, 459–462. [[CrossRef](#)]
5. Ignat'ev, A.I.; Nashchekin, A.V.; Nevedomskii, V.M.; Podsvirov, O.A.; Sidorov, A.I.; Solov'ev, A.P.; Usov, O.A. Formation of silver nanoparticles in photothermorefractive glasses during electron irradiation. *Tech. Phys.* **2011**, *56*, 662–667. [[CrossRef](#)]
6. Popov, V.V.; Basteev, A.V.; Solovey, V.V.; Prognimak, A.M. The effect of metal-hydride activation of hydrogen and investigation of its influence on the characteristics of gas-discharge hydrogen-using energy conversion devices. *Int. J. Hydrog. Energy* **1996**, *21*, 259–265. [[CrossRef](#)]
7. Prognimak, A.M. Mass-spectrometry investigation on the effect of metal-hydride activation of molecular hydrogen. *Int. J. Hydrog. Energy* **1995**, *20*, 449–453. [[CrossRef](#)]
8. Aliotta, M.; Raiola, F.; Gyürky, G.; Formicola, A.; Bonetti, R.; Broggin, C.; Campajola, L.; Corvisiero, P.; Costantini, H.; D'Onofrio, A.; et al. Electron screening effect in the reactions $3\text{He}(d,p)4\text{He}$ and $d(3\text{He},p)4\text{He}$. *Nucl. Phys. A* **2001**, *690*, 790–800. [[CrossRef](#)]

9. Lipson, A.G.; Roussetski, A.S.; Karabut, A.B.; Miley, G. Strong Enhancement of DD-reaction and Soft X-ray Generation in a High-current Deuterium Glow Discharge at Voltages 0.8-2.5 keV. *J. Exp. Theor. Phys.* **2005**, *100*, 1334–1349. [[CrossRef](#)]
10. Chan, C.T.; Louie, S.G. Self-consistent pseudopotential calculation of the electronic structure of PdH and Pd₄H. *Phys. Rev. B* **1983**, *27*, 3325–3337. [[CrossRef](#)]
11. Nechaev, I.A.; Zhukov, V.P.; Chulkov, E.V. Ab initio calculation of the lifetime of quasiparticle excitations in transition metals within the framework of the GW approximation. *Phys. Solid State* **2007**, *49*, 1811–1819. [[CrossRef](#)]
12. Chernov, I.P.; Larionov, V.V.; Lider, A.M.; Maximova, N.G. Energy storage using palladium and titanium targets. *Indian J. Sci. Technol.* **2015**, *8*, 1–5. [[CrossRef](#)]
13. Lee, J.Y.; Lee, S.M. Hydrogen trapping phenomena in metals with BCC and FCC crystals structures by the desorption thermal analysis technique. *Surf. Coat. Technol.* **1986**, *28*, 301–314. [[CrossRef](#)]
14. Podsiadły-Paszkowska, A.; Krawiec, M. Tuning the Electronic Structure of Hydrogen-Decorated Silicene. *Condens. Matter* **2017**, *2*, 1. [[CrossRef](#)]
15. Chernov, I.P.; Larionov, V.V.; Lipson, A.G.E.; Tyurin, Y.I. Production of high-energy deuterons upon electron-beam excitation of deuterium-saturated palladium. *High Temp.* **2010**, *48*, 599–602. [[CrossRef](#)]
16. Larionov, V.V.; Nikitenkov, N.N.; Tyurin, Y.I. Hydrogen diffusion in steels under electron bombardment. *Tech. Phys.* **2016**, *61*, 793–797. [[CrossRef](#)]
17. Bordulev, Y.S.; Laptev, R.S.; Kudiiarov, V.N.; Lider, A.M. Investigation of commercially pure titanium structure during accumulation and release of hydrogen by means of positron lifetime and electrical resistivity measurements. *Adv. Mater. Res.* **2014**, *880*, 93–100. [[CrossRef](#)]



© 2018 by the authors. Licensee MDPI, Basel, Switzerland. This article is an open access article distributed under the terms and conditions of the Creative Commons Attribution (CC BY) license (<http://creativecommons.org/licenses/by/4.0/>).